Study on the Improvement of the Electrochemical Characteristics of Surface-modified V-Ti-Cr alloy by Ball-milling

Jin-Ho Kim, Sang-Min Lee, Ho Lee, Paul S. Lee, and Jai-Young Lee

Department of Materials Science and Engineering,
Korea Advanced Institute of Science and Technology,
373-1 Kusong-Dong, Yusong-Gu, Taejon, South Korea

Abstract

Vanadium based solid solution alloys have been studied as a potential negative electrode of Ni/MH battery due to their high hydrogen storage capacity. In order to improve the kinetic property of V-Ti alloy in KOH electrolyte, the ball-milling process with Ni, which has a catalytic effect of hydrogen absorption/desorption, was carried out to modify the surface properties of V-Ti-Cr alloys with high hydrogen storage capacity. Moreover, to overcome the problem of poor cycle life, V-Ti alloy substituted by Cr, V0.68 Ti0.20 Cr0.12, has been developed showing a good cycle performance (keeping about 80 % of initial discharge capacity after 200 cycles). The cycle life of surface-modified V0.68 Ti0.20 Cr0.12 alloy was improved by suppressing the formation of TiO2 layer on the alloy surface while decreasing the amount of dissolved vanadium in the KOH electrolyte. In order to promote the effect of Ni coating on the surface property of V0.68 Ti 0.20 Cr 0.12 alloy by ball-milling, filamentary-typed Ni, which has higher surface coverage area than sphere-typed Ni was used as a surface modifier. Consequently, the surface-modified V0.68 Ti0.20 Cr0.12 alloy electrode showed a improved discharge capacity of 460 mAh/g.

Jin-Ho Kim, Sang-Min Lee, Ho Lee, Paul S. Lee, and Jai-Young Lee

1. Introduction

Vanadium based solid solution alloy containing titanium is attractive for an anode material in Ni/MH secondary battery due to its large hydrogen storage capacity in gas/solid reaction. [1] However, the V-based alloy was inactive for electrochemical applications because of its poor electrocatalytic activity. [1] Recently, it was found by some groups that the discharge property was greatly improved by partial substitution by Ni, which act as a catalyst for hydriding and dehydriding. [2-3] Tsukahara et al. have found that the Ni-substituted Ti-V-Ni system alloys have the improved electrochemical kinetics. However, the Ti-V-Ni alloys showed a drastic degradation of hydrogen storage capacity owing to the formation of TiNi second phase, which has a non-hydriding property, caused by substitution of Ni. Kim et al. [4] have reported that the V0.9Ti0.1 alloy and Ni powder have been sintered to modify the surface of alloy by providing a catalytic Ni layer on the surface, but it was also found that the hydrogen storage capacity is decreased by the VNi3 phase, which has a non-hydriding property, formed by high sintering temperature (900℃). Recently, Kim et al. [5] reported that the ball-milling process was effectively employed to modify the surface property of V-Ti alloy with Ni powder because it did not change the bulk properties of the alloy and showed a high discharge capacity of 438 mAh/g. Therefore, the

ball-milling process can be expected as a promising method for the surface-modification.

Although the electrochemical property of the V-base alloy was improved by the addition of Ni, it usually appeared that its discharge capacity rapidly decreased during charge-discharge cycling. [2-3] The rapid degradation of the V-based alloy electrode with cycling was ascribed to the dissolution of V and Ti (mainly V) from the near surface region into the electrode and the formation of TiO2 layer on the alloy particle surface. [6] Therefore, the drastic decay of the alloy electrode should be overcome for the application of the V-based alloy system to a Ni-MH battery. Yu et al. [7] reported that Cr-substitution in Ti-based alloy electrode improved the cycle-life of the electrode by restraining the dissolution of V in KOH solution and preventing the formation of TiO2 layer caused by the dense Cr2O3 layer. Therefore, Cr-substitution can be considered to be an effective method in improving the cycle-performance of V-based alloy electrode.

Recently, Yu et al. [8] also reported that the surface-modification using the flake-shaped Ni instead of sphere-shaped Ni increased more the discharge capacity of Ti-based alloy electrode. And it is also known that the surface coverage area of flake-typed powder is larger than that of sphere-shaped powder. Therefore, it may be expected that the surface-modification with any Ni powder, whose surface area is larger than that of

flake-typed Ni, will be very effective in improving discharge capacity.

In the current study, we carried out the Cr-substitution for the improvement of the cycle performance of V-Ti alloy with high reversible storage capacity of 2.0wt%, and investigated the effect of Cr-substitution in V-Ti alloy. Also we carried out the surface-modification of V-Ti-Cr alloy by ball-milling with various Ni, such as sphere-typed Ni, flake-typed Ni and filamentary-typed Ni, to improve the electrocatalytic activity and discharge efficiency of V-Ti-Cr alloy.

2. Experimental

V $0.87-X$ -Y Ti $0.13+Y$ Cr X (X= 0 0.15) (Y= 0 0.09) alloys were prepared by arc melting in an argon atmosphere. The alloys were turned over and re-melted several times to obtain a homogeneous structure. The as-cast samples were pulverized by repeated hydrogenation reaction to prepare powder below 100 mesh.

The surface of the V0.87-X-YTi0.13+YCrX alloy powders was modified by ball-milling with the various types of Ni powders in an argon atmosphere. V0.87-X-YTi0.13+YCrX alloy powder and Ni powder were mixed together in the various weight ratio (10, 9, 8, 7, 6 wt.% Ni per alloy), followed by ball-milling at a vibrating speed of 500 rpm for 40, 30, 25 and 20 min to prepare the active alloy powders. Fig. 1 shows the schematic diagram of the surface-modified V-Ti-Cr alloy powders with Ni. Also, in this research, three

types of Ni powder (sphere-shaped Ni, flake-shaped Ni and filamentary-shaped Ni), which have different surface area respectively, were prepared as modifier. Fig 2. shows the SEM images with the morphology of various Ni powders. The filamentary-shaped Ni (Inco type 210H Extra Fine Nickel Powder) has the largest surface area and sphere-shape Ni has the smallest it.

The active alloy powder (0.2g) was mixed with Cu powder (0.1g) in weight ratio of 2:1 and pressed at 10 ton/cm2 to form a pellet of 10 mm in diameter. A half-cell was constructed using Pt wire as a counter electrode and a mercury/mercury oxide (Hg/HgO) electrode as a reference in the 6M KOH electrolyte. The alloy electrode was charged at 100 mA/g for 6h; after resting for 5 min it was discharged at 30 mA/g until its potential reached 0.75 V (vs. Hg/HgO) at 303 K.

The structure and lattice parameters were measured using an X-ray diffractometer (Cu K radiation). In order to investigate the gaseous hydrogenation characteristics of alloys, pressure-composition-isotherm (P-C-Isotherms) curves were measured by an automatic Sieverts type apparatus at 303 K. To investigate the surface morphology and concentration profiles of the electrodes before and after the charging-discharging cycles, scanning electron microscopy (SEM) and auger electron spectroscopy (AES) analyses were performed. The electrolyte solution in the test cells was analyzed after cycle

tests by inductively coupled plasma (ICP) in order to determine the contents of dissolved elements. Electrochemical impedance spectra (EIS) analysis was made on the electrode of DOD (depth of discharge) 50 % at various stages of cycling. The polarization curve was measured in order to examine the corrosion property of electrode by using an EG&G 273A potentiostat.

3. Results and Discussion

Alloy Design of V0.87-X Y Ti 0.13+Y Cr X (X= 0 ~ 0.15) (Y= 0 ~ 0.09) alloys Figure 3 shows the PCT desorption curves of V 0.87-X Ti 0.13 Cr X (X= 0, 0.05, 0.08, 0.12, 0.15) alloys. It appears that the equilibrium hydrogen pressure increases, but the reversible hydrogen storage capacity in 0.01 to 1 atm range of equilibrium hydrogen pressure decreases with increasing Cr mole fraction (X). To investigate the effect of Cr substitution on the cycle-life of V-Ti-Cr electrodes, the discharge curves at 30℃ for V 0.87-X Ti 0.13 Cr X (X= 0, 0.05, 0.08, 0.12, 0.15) alloys were measured and shown in Fig. 4. The ball-milling condition applied to the charge-discharge test was 20 min (ball-milling time) and 10 wt% (Ni content), which is not optimum but tentative. It is observed that the discharge capacity of V 0.87-X Ti 0.13 Cr X (X= 0, 0.05, 0.08, 0.12, 0.15) alloy electrodes were gradually decreased, which was expected from PCT results, but the cycle-life improved with increasing Cr content (X=0

~ 0.12). The Cr substitution of over 12 at%, however, resulted in the degradation of cycle performance. In order to explain such a degradation of cycle performance, XRD and SEM analysis were conducted. From the XRD profiles shown in Fig. 5, it was observed that the alloys with less than 15 at % Cr had a BCC single phase as usually observed in previous work. However, the formation of V-Cr second phase was identified from SEM images of V 0.87-X Ti 0.13 Cr X (X= 0, 0.05, 0.08, 0.12, 0.15) alloys as shown in Fig. 6. For the alloy with more than 15 at% Cr, the V-Cr second phase was observed along grain boundary. Recently, Lee et al. [9] reported that the selective corrosion and dissolution of second phase by Galvanic-Coupling effect lead to the deterioration of Zr-based alloy. Therefore, the degradation of cycle-life, which was observed in V-Ti-Cr electrode over 15 at% Cr, was caused by the V-Cr second phase along grain boundary. Therefore, it was tentatively concluded that the optimum amount of Cr substituted for V is 12 at% Cr and its composition is V0.75 Ti0.13 Cr0.12 alloy.

Figure 7 shows the PCT curves of V 0.75-Y Ti 0.13+Y Cr 0.12 (Y = 0, 0.03, 0.05, 0.07, 0.09) alloys for various Ti contents at 30℃. As shown in the previous experiments, Cr-substitution for V in V-Ti-Cr alloys caused a decrease of reversible hydrogen storage capacity and discharge capacity. In order to retrieve such a reduction in capacity, the atomic ratio of V/Ti was altered. It appeared that the equilibrium hydrogen pressure

decreased and the reversible hydrogen-storage capacity increased with increasing Ti-content substituted for V. However, it was observed that the reversible hydrogen-storage capacity with more than Y=0.07 was already saturated at the value of 2 wt% H. Figure 8 shows the discharge curves for V 0.75-Y Ti 0.13+Y Cr 0.12 (Y = 0, 0.03, 0.05, 0.07, 0.09) alloy electrodes with respect to the substituted Ti contents at 30°C. The ball-milling condition applied to the charge-discharge test was also 20 min (ball-milling time) and 10 wt% (Ni content). As Ti content substituted for V increased to 0.07, the good cycle performance was maintained, while the discharge capacity increases. However, the discharge capacity of V0.66 Ti0.22 Cr0.12 alloy electrode, with Y=0.09, did not increase but rather decreased, as expected from above PCT curves. Therefore, it is concluded that the optimum amount of Ti content substituted for V is 0.07 at% Ti. Consequently, the V0.68 Ti0.20 Cr0.12 alloy with high reversible storage capacity (2.0 wt% H) and good cycle performance has been developed by the substitution of Cr and Ti for V in the V0.87 Ti0.13 alloy.

Surface modification of V0.68 Ti0.20 Cr0.12 alloy by ball-milling with various Ni-powder Figure 2 showed the SEM images of various Ni-powders with different surface coverage areas. It is observed that the filamentary Ni powder has the largest surface coverage area, 7.18 m2/g, compared to the sphere and flake-shaped Ni powder. In order to identify the effect of Ni powder with large surface area, the discharge capacity of surface-modified V0.68 Ti 0.20 Cr 0.12 alloy by ball-milling with different Ni-powders was measured and shown in Fig. 9. It is shown that the ball-milled alloy with filamentary-shaped Ni powder has higher discharge capacity than that of Ni powder with other shapes. It means that the filamentary-shaped Ni powder has effective role in improving the discharge efficiency. For the sake of further increase in the discharge capacity, the optimization of ball-milling conditions (ball-milling time, and Ni content) was carried out for filamentary-shaped Ni. Figure 10 (a) and (b) show the changes of discharge capacity with respect to Ni content and ball-milling time, respectively. The highest discharge capacity of 460 mAh/g was obtained at 7 wt% of Ni-content, and 25min of ball-milling time, which were the optimized ball-milling condition in this work. The Auger electron spectroscopy (AES) analysis, as shown Fig.11, was performed to identify the Ni concentration on the alloy surface, which is supposed to be a major factor to increase the discharge efficiency. It was observed that the Ni concentration of an ball-milled V0.68 Ti 0.20 Cr 0.12 alloy electrode was only enriched on the surface of the alloy, but not in the bulk, demonstrating that the V-Ti-Cr metal particles were effectively lapped with Ni powder.

Measurement of cycle Life for the

ball-milled V0.68 Ti 0.20 Cr 0.12 alloy electrode with filamentary type Ni The cycle life for the ball-milled V0.68 Ti 0.20 Cr 0.12 alloy electrode with filamentary-shaped Ni is graphically illustrated in Fig. 12. The cycle life of the electrode remains about 80 % of its initial discharge capacity, which shows a considerably improved cycle performance than the conventional V-Ti electrodes. The cyclic improvement of surface-modified V0.68 Ti0.20 Cr0.12 alloy was due to the suppressing of formation of TiO2 layer on the alloy surface and the decreasing the amount of dissolved vanadium in the KOH electrolyte. In order to examine more accurate cause of cyclic improvement, the polarization curves of V0.68 Ti 0.20 Cr 0.12 and V0.66 Ti0.22 Ni0.12 alloy electrode in KOH electrolyte were measured and shown in Fig 13. The open circuit potential (O.C.P) of V0.68 Ti0.20 Cr0.12 alloy electrode is 0.656 V (vs. Hg/HgO) and that of V0.66 Ti0.22 Ni0.12 alloy electrode is 0.894 V (vs. Hg/HgO). This means that the corrosion-resistance of V0.68 Ti0.20 Cr0.12 alloy electrode is superior to that of the conventional V-Ti electrodes. Moreover, the O.C.P of V0.68 Ti0.20 Cr0.12 alloy electrode is more cathodic than the working voltage region of Ni-MH battery (-0.75 ～ -1.2V), which also indicates a predominant corrosion-resistance. Based on the polarization analysis, it can be expected that the dissolution of electrode constituents, especially vanadium, in KOH electrolyte will remarkably decrease.

Table 1. shows the results of ICP analysis of V0.68 Ti0.20 Cr0.12 and conventional V-Ti-Ni alloy [10] electrodes in KOH electrolyte with 100 and 30 cycling, respectively. It seems that the amount of vanadium dissolved in KOH solution decreased markedly in spite of extended cycling compared with that of V0.66 Ti0.22 Ni0.12 alloy electrode. Consequently, the cycle life of V0.68 Ti 0.20 Cr 0.12 alloy electrode has been improved because of the suppression of vanadium dissolution in KOH electrolyte.

The area normalized EIS analysis was carried out to identify the degradation behavior of V0.68 Ti 0.20 Cr 0.12 and Ni-coated V0.66 Ti0.22 Ni0.12 alloy electrode by the formation of TiO2 layer on the surface of the alloy. Figure 14 shows that the increasing rate of charge transfer resistance of V0.68 Ti 0.20 Cr 0.12 alloy electrode with cycling decreased compared to that of Ni-coated V0.66 Ti0.22 Ni0.12 alloy electrode, which means the surface property of alloy was improved. As a result, it may be expected that the formation of TiO2 layer on the surface of alloy will be suppressed. AES measurements were performed to investigate the existence of TiO2 layer. Figure 15 shows that the oxygen concentration on the surface of V0.68Ti0.20Cr0.12 alloy electrode decreases markedly compared to the Ni-coated V 0.66 Ti 0.22 Ni 0.12 alloy electrode. This means that the formation of TiO2 layer on the surface is suppressed by substitution of Cr and the cycle life of V0.68 Ti 0.20 Cr 0.12 alloy electrode has

greatly improved.

4. Conclusions

To improve the kinetic property of V-Ti alloy with high hydrogen storage capacity in KOH electrolyte, the ball-milling process with Ni was carried out to modify the surface property of the alloy. Moreover, in order to improve the cycle-life performance of surface-modified $V_{0.87}$ $Ti_{0.13}$ alloy, vanadium was substituted with Cr. It was shown that the cycle-life performance was markedly improved, but the reversible hydrogen storage capacity and discharge capacity were gradually decreased with increasing Cr-content. Accordingly, to increase the reversible hydrogen storage capacity of the V-Ti-Cr alloy, the V/Ti ratio in alloy was controlled. As a consequence, the $V_{0.68}$ Ti 0.20 Cr 0.12 alloy with high reversible hydrogen storage capacity of 2.0wt% and long cycle life (keeping about 80 % of initial discharge capacity after 200 cycles) has been developed. The improvement of cycle life of surface-modified V 0.87 Ti 0.13 alloy was ascribed to the decrease in the amount of dissolved vanadium in the KOH electrolyte and the suppression of the formation of TiO_2 layer on the surface by substitution of Cr. Furthermore, in order to promote the effect of Ni coating on the surface property of V0.68 Ti 0.20 Cr 0.12 alloy by ball-milling, filamentary-shaped Ni with higher surface coverage area rather than sphere-shaped Ni was used

as modifier and the improved discharge capacity of 460 mAh/g has been obtained.

5. Reference

[1] J.F. Lynch, A.J. Maeland and G.G. Libowitz, *Z. Phys. Chem.,* **145** (1985) 51.

[2] M. Tsukahara, K. Takahashi, T. Mishima, T. Sakai, H. Miyamura, N. Kuriyama and I. Uehara, *J. Alloy Comp.,* **226** (1995) 203

[3] M. Tsukahara, K. Takahashi, T. Mishima, T. Sakai, H. Miyamura, N. Kuriyama and I. Uehara, *J. Alloy Comp.,* **224** (1995) 162

[4] D.M. Kim, K.Y. Lee, J.Y. Lee, *J. Alloy Comp.,* **231** (1995) 650

[5] S.H. Kim, S.M. Lee, P.S. Lee, J.Y. Lee, *submitted to J. Electrochem. Soc.*

[6] J.W. Kim, S.M. Lee, H.H. Lee, D.M. Lee, J.Y. Lee, *J. alloy Comp.,* **255** (1997) 248

[7] J.S. Yu, S.M. Lee, K. Cho, J.Y. Lee, *J. Electrochem. Soc.,* **147** (2000) 2013

[8] J.S. Yu, H. Lee, P.S. Lee, J.Y. Lee, *submitted to J. Electrochem. Soc.*

[9] H.Lee, S.M. Lee, J.Y. Lee, *J. Electrochem. Soc.,* **146** (1999) 3666

[10] Q.A. Zhang, Y.Q. Lei, X.G. Yang, Y.L. Du. Q.D. Wang, Int. *J. Hydrogen Energy,* **25** (2000) 977
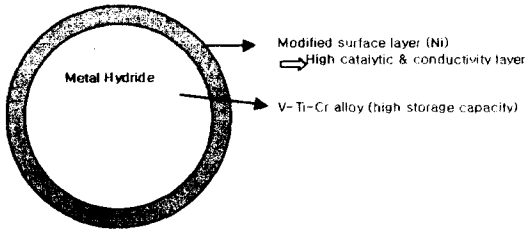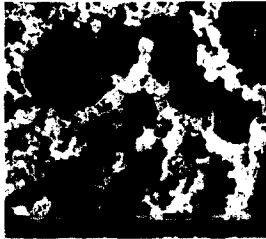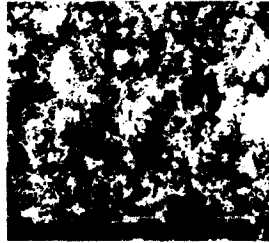
Fig. 1. The schematic diagram of the surface-modified V-Ti-Cr alloy powders with Ni

(a)

(b)   (c)

Fig. 2. SEM images and surface area of various Ni. (a) Sphere-typed Ni powder (0.0127 m2/g), (b) Flake-typed Ni powder (0.542 m2/g), (c) Filamentary-typed Ni powder (7.18 m2/g)
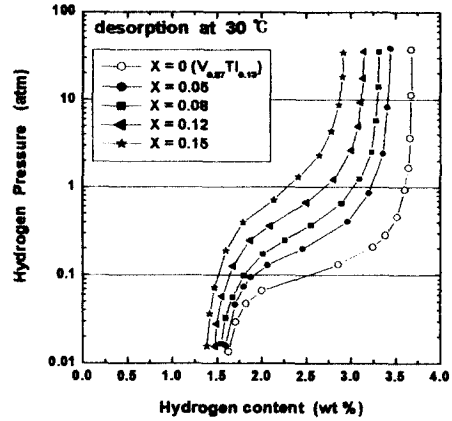

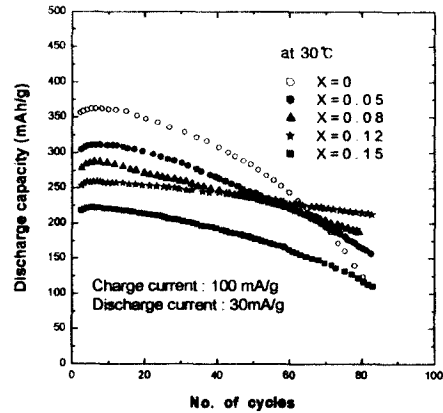Fig. 3. PCT desorption curves of V 0.87-X Ti 0.13 Cr X (X= 0, 0.05, 0.08, 0.12, 0.15) alloys

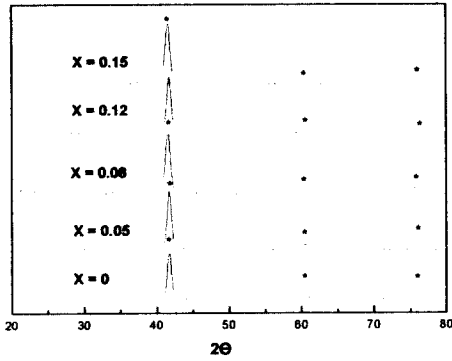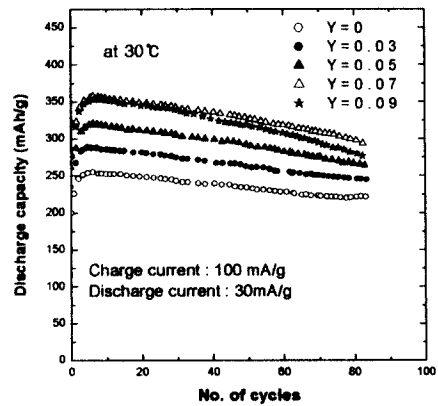Fig. 4. The discharge curves at 30℃ for V 0.87-X Ti 0.13 Cr X (X= 0, 0.05, 0.08, 0.12, 0.15) alloys

Fig. 5. XRD patterns of V 0.87-X Ti 0.13 Cr X (X= 0, 0.05, 0.08, 0.12, 0.15) alloys
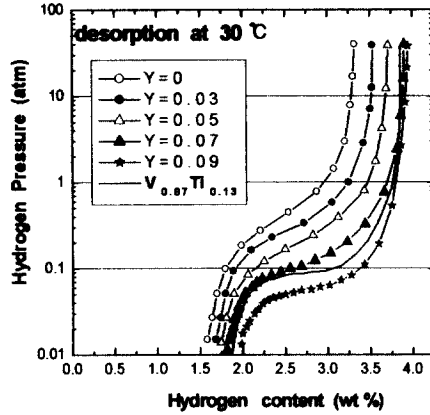
Fig. 7. The PCT desorption curves of V 0.75-Y Ti 0.13+Y Cr 0.12 alloys (Y = 0, 0.03, 0.05, 0.07, 0.09) for various Ti contents at 30℃
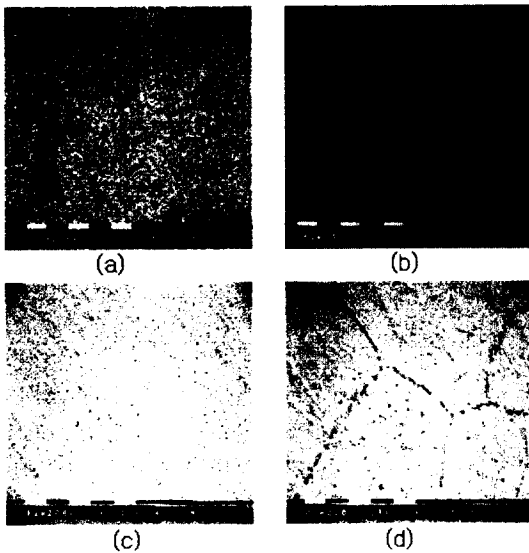
Fig. 6. SEM images of V 0.87-X Ti 0.13 Cr X (a) X = 0 , (b) X = 0.08 , (c) X = 0.12 , (d) X = 0.15 alloys

Fig. 8. The discharge curves at 30℃ for V 0.75-Y Ti 0.13+Y Cr 0.12 (Y = 0, 0.03, 0.05, 0.07, 0.09) alloy electrodes with respect to the substituted Ti content
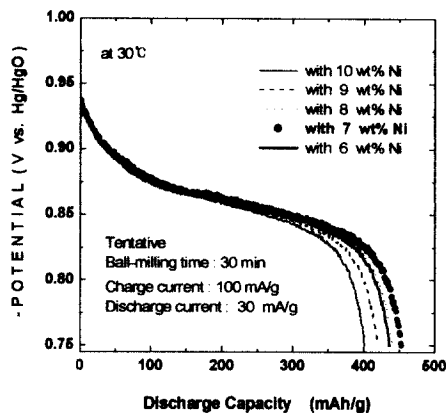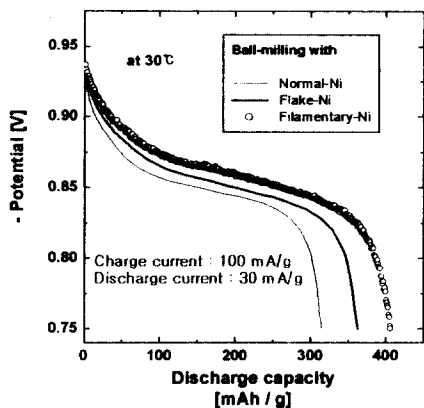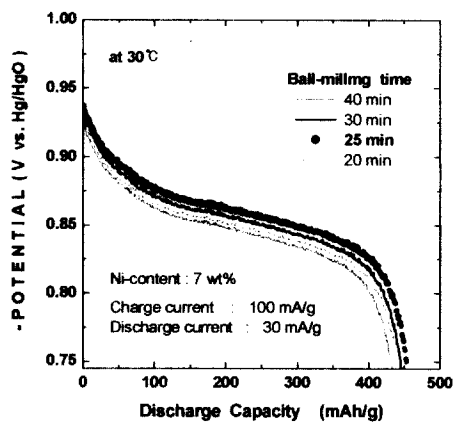
Fig. 9. The discharge capacity of ball-milled alloys with various Ni powder

(a)

(b)

Fig. 10. The optimization of ball-milling conditions (ball-milling time, and Ni content) with filamentary typed Ni (a) Ni-content. (b) ball-milling time
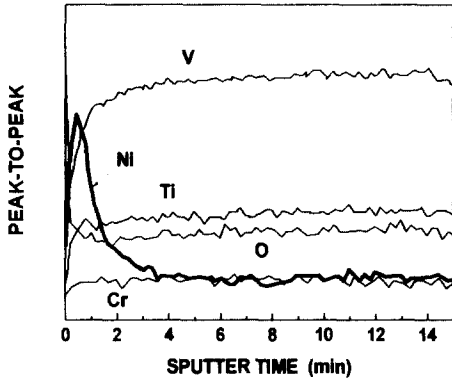
Table. 1. ICP analysis of V0.68 Ti0.20 Cr0.12 and conventional V-Ti-Ni alloy electrode in KOH electrolyte with 100 and 30 cycling   (g/cm^3)

	V 3 Ti Ni 0.56 Hf 0.24 Mn 0.15 Cr 0.3 (after 30 cycles) [Q.A. Zhang et al.]	V 0.68 Ti 0.20 Cr 0.12 (after 100 cycles)
V	94.5	15.6
Ti	2.2	2.0
Ni	5.6	4.9
Cr	0.5	1.6
Hf	0.7	–
Mn	1.4	–

Fig. 11. AES depth profiles of V0.68Ti 0.20Cr 0.12 alloy after ball-milling with filamentary typed Ni
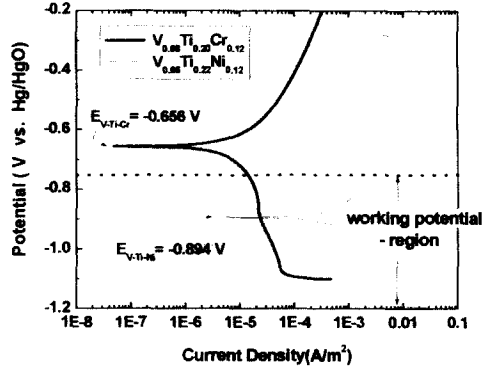
Fig. 13. The polarization curves of V0.68 Ti 0.20 Cr 0.12 and V0.66 Ti0.22 Ni0.12 alloy electrode in KOH electrolyte
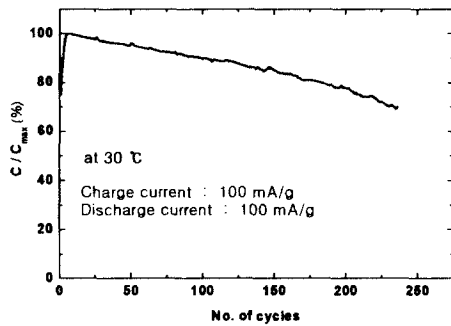

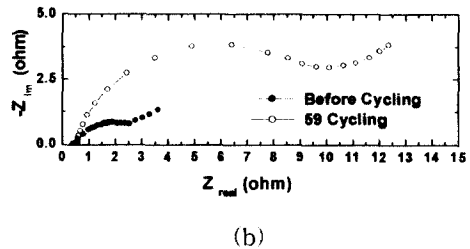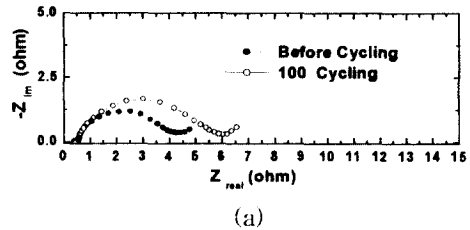Fig. 12. The cycle-life for the ball-milled V0.68 Ti 0.20 Cr 0.12 alloy electrode with filamentary typed Ni

(a)

(b)
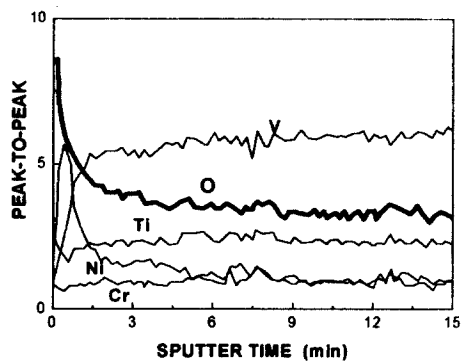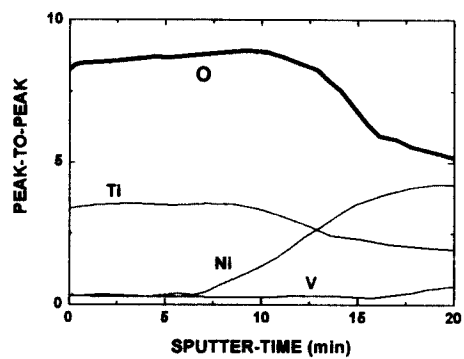
Fig. 14. The area normalized EIS analyses of (a) V0.68 Ti 0.20 Cr 0.12 and (b) Ni-coated V0.66 Ti0.22 Ni0.12 alloy electrode

(a)

(b)

Fig. 15. AES depth profiles of the alloys with cycling (a) V0.68Ti 0.20Cr 0.12 and (b) Ni-coated
V0.66 Ti0.22 Ni0.12 alloy electrode